Stereoscopy for visual simulation of materials of complex appearance

Fernando E. da Graça, Alexis Paljic, Dominique Lafon-Pham, Patrick Callet

Stereoscopy for Visual Simulation of Materials of Complex Appearance.

Fernando da Graça[a], Alexis Paljic[a], Dominique Lafon-Pham[b], and Patrick Callet[a, c]

[a]Robotics Center, Mines ParisTech, 60 Boulevard Saint-Michel, 75006 Paris, France;
[b]Centre des Matériaux, Ecole des Mines d'Alès, 2 Avenue Pierre Angot, Pau 64053, France;
[c]Applied Mathematics and Systems Laboratory, Ecole Centrale de Paris, France;

ABSTRACT

The present work studies the role of stereoscopy on perceived surface aspect of computer generated complex materials. The objective is to investigate if, and how, the additional information conveyed by the binocular vision affects the observer judgment on the evaluation of flake density in an effect paint simulation. We have set up a heuristic flake model with a Voronoï modelization of flakes. The model was implemented in our rendering engine using global illumination, ray tracing, with an off axis-frustum method for the calculation of stereo pairs. We conducted a user study based on a flake density discrimination task to determine Perception Thresholds (JNDs). We obtained small JNDs variations when expressed on Weber fractions: 3.62%, and 3.45% for the monoscopic- and for the stereoscopic-condition. Our results are discussed on the basis of the flake density scale obtained by morphology image processing techniques.

Keywords: virtual reality, predictive rendering, complex materials, metallic paints, stereoscopy, perception threshold

1. INTRODUCTION

Predictive Rendering, as opposed to believable rendering, is a field of research that aims at creating physically correct computer images of materials.[1] The objective is to predict the visual appearance of a material from a model of its composition. If such a tool was to be mastered, it would allow to design a virtual material and simulate its visual appearance iteratively. Then, when the desired appearance is obtained for the virtual material, the actual prototype could be produced, with the set of parameters used as the input for the model. This process is meant to lead to better design at a lower cost. Predictive rendering has a very strong potential in various application domains, from manufacturing industries (automotive, aeronautics), cosmetics (creams, make-up) to architecture (material design), to cite a few.

On the other hand, Virtual Reality (VR) is used in the industry for product design or industrial process validations. Through the use of stereoscopic displays, user motion capture, motion parallax, VR allows for a user to feel immersed in a 1:1 scale virtual environment, and to observe objects and interact with them. In particular, binocular vision and motion parallax are necessary to provide the human visual system with valuable depth and shape cues. These are key characteristics of VR that are necessary to ensure "human in the loop" simulations. In order to combine the physical and visual validity of Predictive Rendering and perception cues provided by Virtual Reality, the need for stereoscopy and motion parallax for predictive rendering simulations is being expressed by the industry.

Predictive rendering approaches require perceptual validations that take into account the human visual system in order to be valid. The field of research for such validations is large and we are only starting to draw the boundaries within which virtual material samples are representative of real material samples. Indeed, image quality perception can depend on a lot of parameters that appear at several stages of the process. One should,

Further author information: (Send correspondence to Fernando da Graça.)
Fernando da Graça: E-mail: fernando.graca@mines-paristech.fr, Telephone: (+33) 01 40 51 94 39
Alexis Paljic: E-mail: alexis.paljic@mines-paristech.fr
Dominique Lafon-Pham: E-mail: dlafon@mines-ales.fr
Patrick Callet: E-mail: patrick.callet@{mines-paristech.fr, ecp.fr}

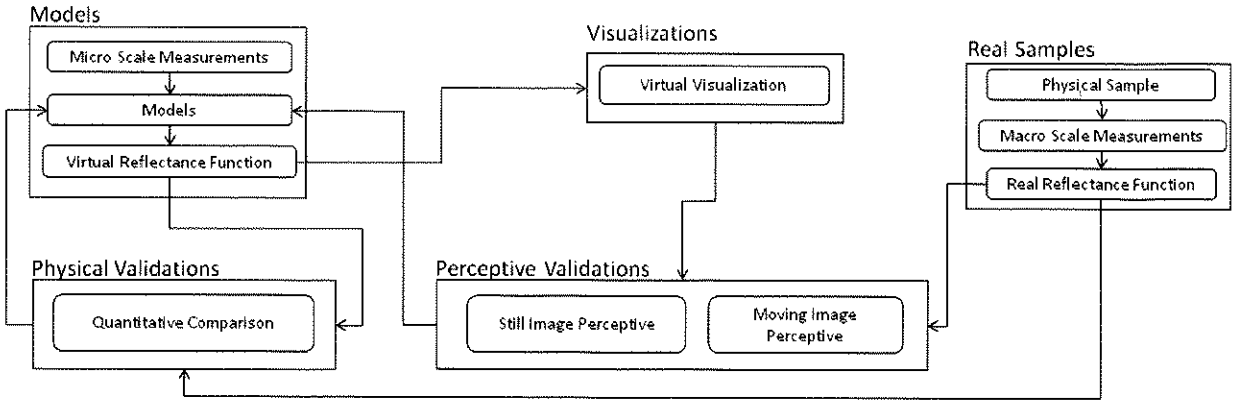

Figure 1. This diagram shows the pipeline used to validate the obtained results of a predictive rendering engine.

at least, consider the following: the human user (visual acuity, individual color perception, visual fatigue), the technical setup (display calibration, display resolution, luminance), the sensory motor inputs and outputs (use of stereoscopy, motion parallax, users ability to manipulate the virtual material sample), and the rendering engine itself (light-matter interaction models, material models).

In this context, this work is part of an iterative, validation process of a predictive rendering engine, see diagram of the figure 1. In the literature, the role of stereoscopy has been studied for perception of macroscopic properties of virtual scenes (depth, object size), however, the influence of stereoscopy on perception of visually small local properties of materials is not well known. In this work we want to focus on the role of stereoscopy in the perception of local characteristics of simulated surfaces. As a working case we will focus on car paint and effect paints that have binocular differences, since the applied research context is car paint design.

We begin the paper with a survey of related work in section 1.2. In section 2 we characterize the heuristic flake model used to simulate plates of different flake density. Then, we describe the experimental setup of the experiment. In the section 3 we present the psychometric results of the measured data. The experimental results are analyzed in the section 4, we also describe the image processing method used to describe the flake density. Finally, in section 5 we present our conclusions, and we address some aspects for future work to complement our findings.

1.1 Objectives

This work is part of a research project* that aims at predicting the visual appearance of materials from models of their microstructure. It involves an understanding, and making of the physical formulation of materials at a nanoscopic-scale . Reflectance functions of materials are computed using models based on homogenizations methods.[2] The final goal is the visualization of virtual materials by a human observer. To this end, it is crucial to do qualitative and quantitative comparisons between the virtual object and its physical counterpart.

1.2 Related Work

In this section, we first propose an overview of the existing computer graphics methods for computer generated (CG) images of materials with nano/macro inclusions such as car paints with flakes. We then explore the existing literature on the role of stereoscopy on the perception of surface aspect.

Figure3(a) shows a cross section of a car paint. Typically the flakes are made of aluminum, and are distributed on the primer surface of the plate at different depths, and the clear coat is transparent. Each flake has a different orientation. The amount, distribution, and the orientation of the flakes are controlled by a milling machine. These metallic pigments convey distinctive visual appearances to the object such as sparkle, and directional

*webpage of the project: lima-project.org

visual effects. The appearance of these nonuniform paints depend on the lighting conditions (direction/diffuse), distance and angle of observation, orientation, diameter and density of the flakes.[3–5]

In the Computer Graphics (CG) domain, several researches have proposed different methods to simulate car paint models. These models are based on Bidirectional Reflectance Distribution Function,[6] which represents how the surface reflects the incident light at different angles. The distribution of the reflectance of the light can be captured by optical measurement devices.[7] Then, the obtained data is used to derive reflectance models that represent the appearance of the physical material.[8]

Generally speaking, we can distinguish two groups: analytical, and data-driven models. In the first, the user tweaks several parameters until he achieves a visual aspect that is similar to the real paint. Durikovic et al.[9] model the geometry of the flakes inside the paint film. Their system is capable of generating stereoscopic images, and it allows to define the parameters for the random distribution of the position of flakes and their orientation. The approach of Ershov et al.[10]is based on reverse engineering, the appearance attributes such gloss are added to the physical model by adjusting parameters. The inconvenient of these models is the amount of parameters that are necessary to represent the car paint appearance.

In the second approach, Günther et al.[11] developed an image based acquisition setup to measure the Bidirectional Reflectance Distribution Function(BRDF) of a car paint. To this BRDF they add the sparkle simulation. The distribution of the the flakes is stored as a texture. Rump et al.[12] used a similar approach as the previous one. The difference is that, instead of using a sparkle simulation with the BRDF, they capture the spatially varying appearance (sparkle effect) using Bidirectional Texture Function (BTF) measurements. In addition, they store and simulate directional visual effects. Sung et al.[13] determine individual flake orientations in the car paint by using confocal laser scanning microscope. They capture the angular dependent reflectance using a goniometer. Then, they use these measurements to built a reflectance model.

In the context of this work, we need to evaluate the perception limits in a VR environment, when the observer perceives the aspect of the reflectance models using binocular vision. The just-noticeable difference (JND) has been used to understand the limitations of the human perception for binocular vision, for instance, in the case of depth perception.[14]

A human observer perceives the binocular summation of the left and right image. In the combination of the two images, we can identify two cases binocular fusion and rivalry. In the first case, if two retinal points are sufficiently similar, a binocular combination occurs. In contrast, when two retinal points are very distinct, the observer perceives a fluctuation between the left and right images, that is, a failed fusion occurs. This phenomenon is known as binocular rivalry.[15]

Most of the work was done on the evaluation of gloss. In the literature the gloss is defined to be a global property of the surface aspect.[16,17] Glossy surfaces reflect the incident light to a particular outgoing direction, which is measured between a specific angular interval (such as -15 degrees to 15 degrees). The perception of specular reflections is an important cue to evaluate the glossiness of the materials. In addition, there is an influence of binocular cues such as highlight disparities on the perception of gloss.[18] The experimental results of Wendt et al.[19]show an improvement of gloss perception when highlights cues disparities are taken into account. The experimental results of the work of G. Obein et al.[20] suggest also that the binocular vision helps for judgment of high gloss samples. They found that with binocular vision the sensitivity to gloss is higher than the monocular vision, for high gloss levels. Sakano et al.[21] examined the effects of the combination of self-motion and contingent retinal-image motion (motion parallax) on perceived glossiness. When the observer moves the head, a stronger glossiness was perceived than when both the observer and the stimulus were static. From their experimental results, they found that the glossiness under the mono condition was underestimated compared to stereo condition. The glossiness under static condition was underestimated compared to dynamic condition. Knill et al.[22]study the combination of different cues for slant perception. At low slants, observers use more the binocular cues than the texture. At slants of 50 and 70, the subjects do better slant judgments using the texture information of the image. As the slant increases the observers give more attention to texture information.

2. USER STUDY

We conducted a user study based on a flake density discrimination task to determine Perception Thresholds (JNDs), and to compare Stereoscopic and Monoscopic Displays. During the experiment, the participants sat in

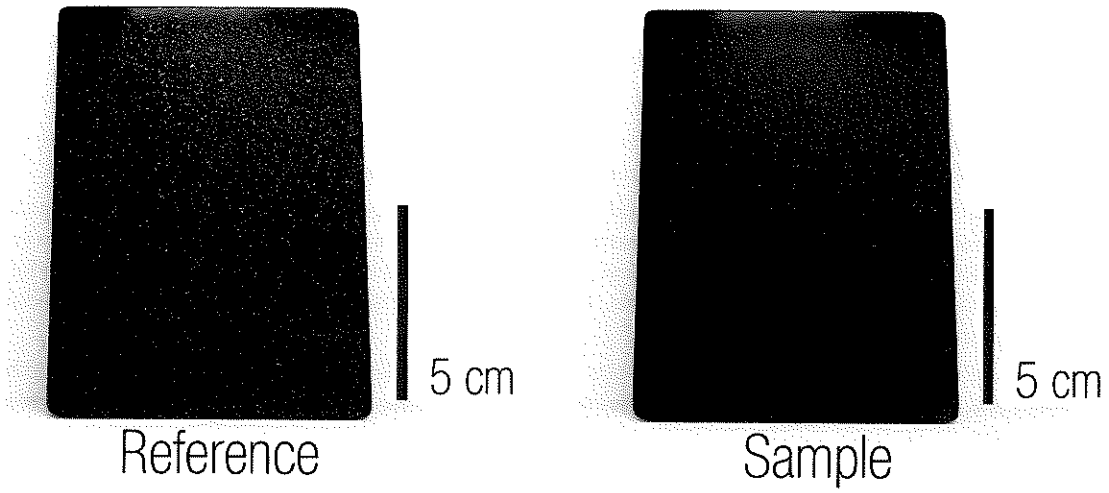

Figure 2. The stimulus displayed to the subjects. The "Reference" material (left plate) is static through the experiment, while the material of the plate "Sample" (right plate) varies randomly showing 20 different densities of flakes.

a dark room covered with black curtains, facing the screen, without any additional lighting. For each trial, the subjects observed series of stereoscopic images of two plates, with different flake density, placed side by side. The plates were presented in random order.

In this work the JND is given by the intensity value with respect to 75% probability that an observer gives a positive answer. Sixteen subjects participated in the experience. All participants had normal or corrected to normal vision, and they did not have previous contact with the experiment. To verify if they perceived stereo depth, prior to the experiment the observers did a stereo-acuity Wirt test, Stereo Fly SO-001.

The main experiment was preceded by a practice trial of two stimuli to gain familiarity with the experience. The subject is asked if the sample plate seems to have more flake density than the reference plate, see figure2. They were told to respond quickly based on their first impression. Subjects were asked to report verbally to the experimenter "More" or "Less" to each visual stimulus. After an answer was given, the operator changed randomly the sample plate while the reference plate remained fixed.

The subjects used stereoscopic active shutter glasses during both monoscopic and stereoscopic conditions. For the monoscopic-condition, the same image was presented for each eye. The images were displayed using an active stereo projector, at a very small throw distance so the pixel density is below Human Visual Acuity for the observation distance of 1m. For each trial, the subjects observed two sequences of 20 stereoscopic images. The first sequence corresponds to the monoscopic-condition, while the second corresponds to the stereoscopic case. For each subject, the order of the stereoscopic-, and monoscopic-condition was randomized.

2.1 Material Simulation

2.1.1 Heuristic model

In order to display metallic flakes, we developed a heuristic model based on the observations of real car paint models. We generate a distribution of flakes, by creating a Voronoï texture. In the same texture, a normal for each flake is randomly generated within an interval of $-10°$ to $10°$ on two axis. This data structure is used in the rendering engine to create the stimuli. Figure3(b) shows an example of the image used as data structure containing both Voronoï distribution of flakes and random normals. The result in the rendering engine mimics the appearance of metallic flakes as in.[23] The flakes are considered isotropic, with mirror like reflection.

The Voronoï model we used modelizes flakes and black background. A segmentation is created, and some areas receive a non null luminance (flake) and some receive a zero luminance (background). We used a single Voronoï segmentation of this 2D space for all stimuli, the consequence of this is that the position of all flakes

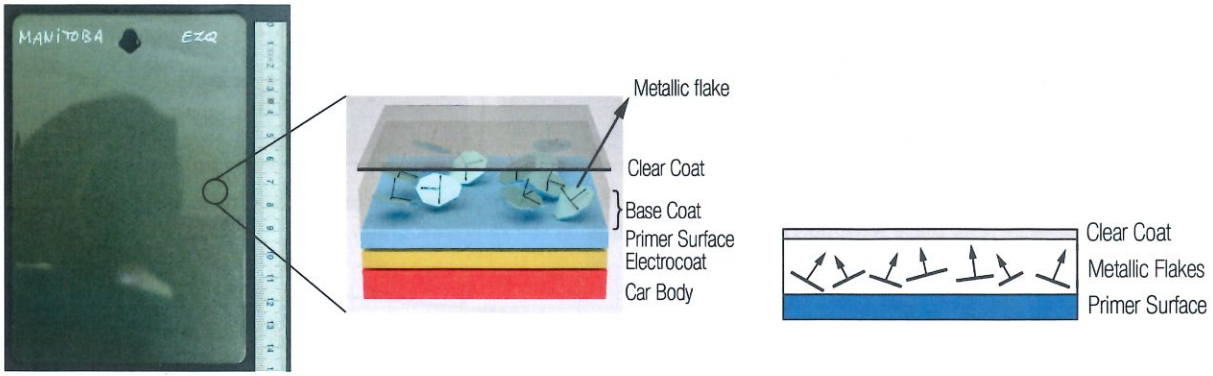

(a) (b)

Figure 3. On the left of the image (a), an example of a real car paint plate. On the right, a diagram of a typical coating paint. The flakes have typically the shape of a disk with a diameter of 5μm to 50μm, in the case of a car paint. The surface can contain rugosity and an interference film. The flakes are imbedded in the base coat with different orientations and depth. The figure (b) depicts the normal orientation of the flakes. For each metallic flake, the x-, y-, and z-axis of the normal vector is registered in the texture using the RGB values of the pixel.

and black background areas remains constant over all stimuli. To create different plates with variable density of flakes, we apply a gain function to the gray levels, which allows to increase or decrease the brightness of the texture. Density increase is obtained by "lighting" black areas (i.e. turning "background flakes" into "metallic flakes". From this heuristic model, we calculate a density metric with an image analysis method that we describe in the next subsection.

In this work we study achromatic plates. We chose to produce gray levels images. We wanted the subjects to concentrate their attention on the perceived reflection highlights of the metallic flakes and not their color. The primer surface of the plate is black. We carefully chose the size of the flakes, in order to have sufficient pixels per flake at a given distance of observation. The size of the flakes used in the virtual 3D scene was chosen in order to have at least 3 pixels per flake i.e. at least a minimum of 0.9mm diameter for a flake. The generated plates have rather large flakes, compared to the ones used in car paints (around 25μm). Our objective was to minimize the influence of rendering filtering methods in the render engine (e.g. box and gaussian filter). Figure 2 shows an example of a rendered plate.

2.1.2 Image Analysis

A priori, we don't know what are the characteristics of the visual signal produced on the screen that are used by the observer's visual system in order to discriminate density.

We must point out that what the human visual system observes here is a visual signal coming from a screen. In other words, the grayscale function doesn't represent directly the geometrical structure, it represents the results of the computer simulation of the interaction between a light source and a model of a complex medium.

For the perceptive comparison by the human visual system of these images, several hypothesis can be done : An average gray level of each image could be used as a density indicator, but also the importance and frequency of clusters of flakes, as well as maximum gray level peaks frequency. Combinations of these characteristics could also be used.

In this subsection we propose an analysis of global properties of the stimulus images that are classically used in the image analysis community.

We focus on three main properties of the stimulus images : size, shape, and height of the gray level peaks corresponding to the optic expression of the displayed flakes.

To that end, we used a classical morphological filter on the gray levels, see figure 6. It consists on successive morphological opening filters with increasing sizes of the structuring isotropic element.[24]

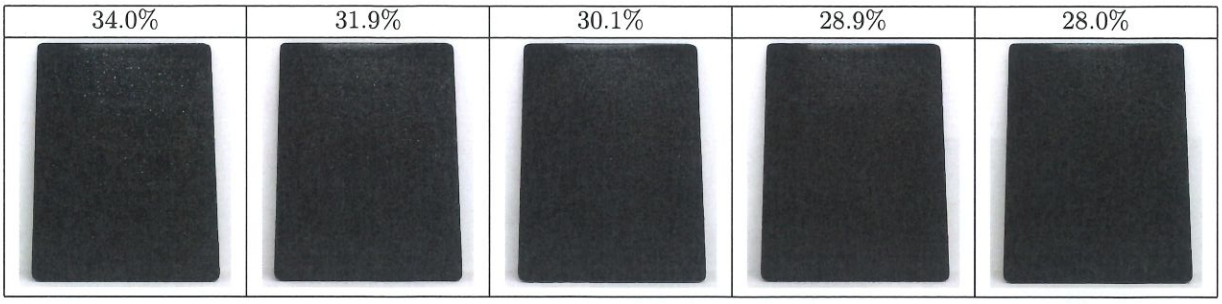

Figure 4. This figure depicts 5 plates of different metallic flake density, from maximum to minimum flake density i.e., from 34.0% to 28.0%. The plate with 30.1% of deleted volume is the reference plate.

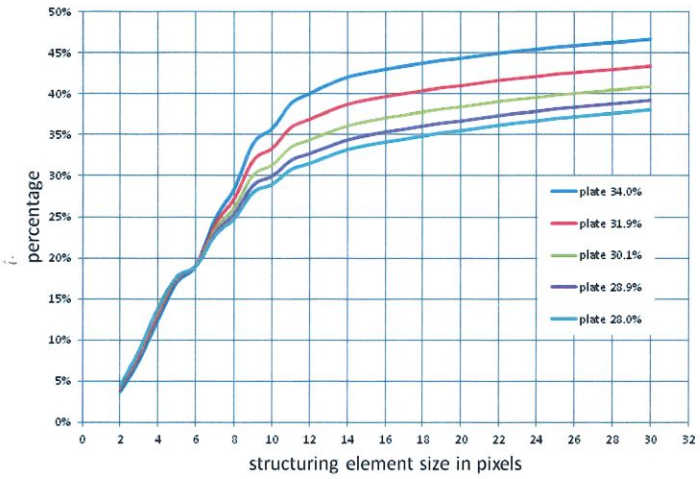

Figure 5. The graph shows the evolution of the gray-function values – obtained from the morphological operations – for 5 different plates. The y-axis represents the percentages of the deleted volume

The morphological filtering is an "opening" operation for the gray levels to evaluate the occupied surface versus the global surface.

From the image analysis we can identify for which opening sizes the gray levels of the plates vary the most, see graph 5. In other words we performed a granolumetric study of the gray function (analysis of the peak of the gray-function).

All plates have the same response in gray level up to a opening size of 6 pixels. This confirms that in our simulation the background remains constant for all plates for this scale. Starting at size 6-pixel to 9-pixel opening, we can consider that all the peaks are characteristic of the presence of at least a flake or a cluster of flakes.

Since, the maximum difference among the shape of the curves is at the 9-pixel opening. We use the corresponding volume percentage as our metric to differentiate the plates.

Figure 5 depicts the evolution of the percentage of the deleted volume, V, versus the opening of the structuring element. In this study, the parameter volume, V, refers to the global appearance of the surface, which is the sum of the gray levels of the plate. The percentage of deleted volume is given by the expression $V = \frac{V_i - V(j)}{V_i}$, which is the difference between the initial volume and the current morphological iteration volume $V(j)$, normalized by the initial volume.

The range of stimulus comprises 20 plates of different flake density from maximum to minimum flake density the percentage of volume is from 34.0% to 28.0%, where the reference plate has 30.1%. Figure 4 shows plates

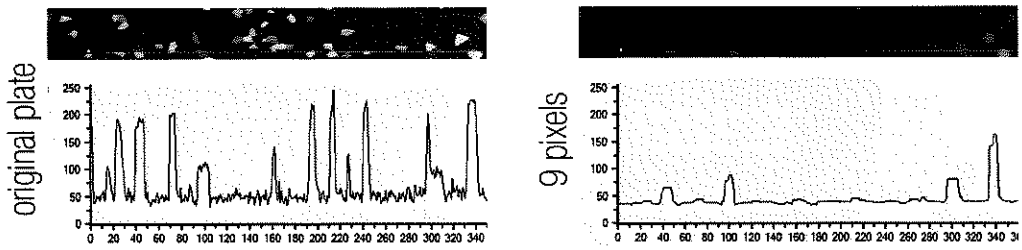

(a) (b)

Figure 6. The profile on the left (a) shows the histogram of a line of pixels on the surface of the plate 1. On the right hand (b) the histogram of the same line after the application of the morphological filtering operation for the size 9-pixel.

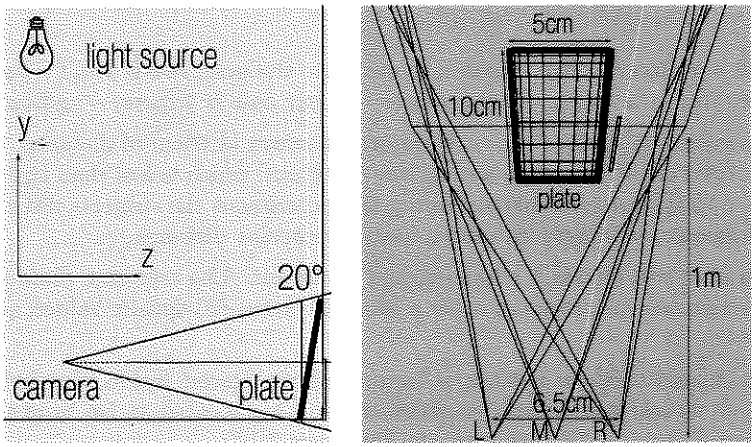

(a) (b)

Figure 7. The images (a) and (b) depict a graphical illustration of the virtual scene. Plate of size 10cm × 5cm × 7mm is placed inside of a lightbooth box of dimensions 1.5m × 1.5m × 1.5m, and it is rotated 20° on x-axis. The distance of observation is fixed at 1m, the light is emitted from the top. For the stereo view we do an off-axis projection. L and R are the position of the left and right camera with intraocular distance of 6.5cm, and M is the position of the cyclopean camera.

among the 20 that were used in the experiment.

2.2 Setup

Figure 7 represent the virtual scene used in the experiments, we use a directional isotropic light, which is emitted from the top of the lightbooth, see figure 7(a). The virtual cameras are placed at a distance of 1m from the plates. The stereo cameras have an interocular distance of 6.5cm and the cyclopean camera is placed in the middle of the left and right cameras, see figure7(b). Figure 8(b) shows the distance of observation, and projection area size used to setup the virtual cameras. The field of view, fov, of the camera was calculated using the observation distance, a, and the width of the area of projection, b, $fov = 2 \times \arctan\left(2a/b\right)$.

In all experiments, the subjects used stereoscopic active shutter glasses NVIDIA 3D Vision 2 during both mono and stereo conditions. For the monoscopic conditions the same image was displayed for both eyes. The stimulus was shown with an active stereo projector with a resolution of 1280 × 720 pixels, capable of showing stereo images at 60Hz. The images are displayed with a rear projection screen. The projector is placed at very small throw distance from the screen, so the pixel density is below Human Visual Acuity.

To increase the pixel density per surface area, we approached the projector to the screen as it is displayed in the figure 8(a). Using the standard human visual acuity of one arcminute, we identified the physical pixel size

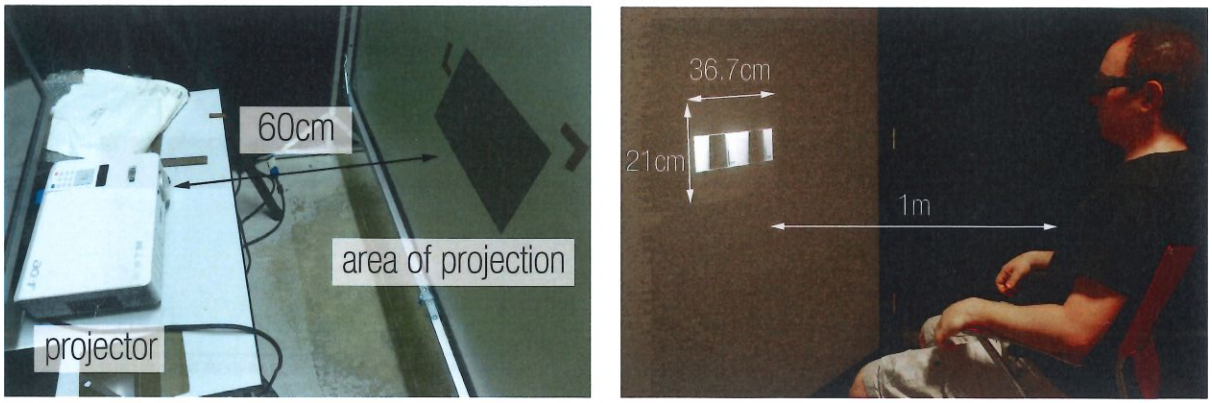

(a) (b)

Figure 8. The images (a) and (b) show the conditions of the experiment. The stimulus was displayed with a rear projection screen. The observer is placed in front of the screen.

that the observers could not discern. The equation to calculate the pixel size is $s = d \times \tan({}^{va}/_{2})$, where s is the pixel size, d the distance from the display to the viewer – in our case is 1 meter – and va is the visual acuity.

The projector is placed in the back of the rear projection screen at 60cm of distance. In these conditions we have a projection area of 36.7cm $\times$ 21cm with a pixel size of 292μm, which is less than the standard visual acuity. The observation distance to the screen is fixed. During the experiment the subjects did not use a chin-rest. For the generation of the stereoscopic images we used a fixed interocular distance.

The stimulus consisted of two plates: a reference, and a variable. The reference plate has a density of 30.1%. For the variable plate, we present in a random order a set of 20 plates (20 density values, see section 2.1.2 "Image Analysis").

The plates have dimensions of 5cm $\times$ 10cm $\times$ 7mm, and are placed inside of a lightbooth of dimensions 1.5m $\times$ 1.5m $\times$ 1.5m. The virtual stereo and cyclopean cameras are located at 1m from the plates, which is the same distance of observation used in the experiments, see figure 7(b).

3. RESULTS

From our experimental findings, see table 1, the obtained JND for the monoscopic and stereoscopic condition is 30.8% and 30.6%. The Weber's fraction value (K = JND/Reference) for the monoscopic condition is 3.62% and for the stereoscopic is 3.45%. From the graph 9 we verify that the point of subjective equality (PSE) is close to the reference plate. This suggests that there were no differences in visual context between reference and sample plates.

The results were obtained by fitting the psychometric function to the recorded data using the probit analysis. To assess the overall performance of the fitting model, we compute the McFadden pseudo R^2. The obtained coefficients for the monoscopic and stereoscopic conditions are 0.8778, and 0.8738.

Table 1.

Condition	JND	Weber Fraction
Mono	30.8%	3.62%
Stereo	30.6%	3.45%

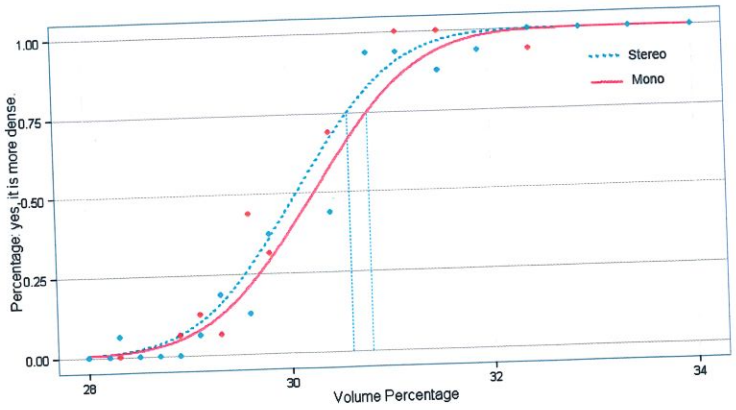

Figure 9. The graph plots the fitted psychometric functions for the monoscopic and stereoscopic cases. The x-axis corresponds to the intensity of the stimulus, the y-axis displays the probability of positive answers i.e., the viewer perceives the "sample" plate denser than the "reference" plate . The intensity of the stimulus corresponds to the value of the gray function of the opening 9 pixels, from more dense to less dense.

4. DISCUSSION

Although we have shown a role of stereo on density perception, the JND does not show a strong variation when expressed as a Weber Fraction.

Several hypothesis are possible to explain this:

1. The metric that we have chosen is not the most representative of the perceptual phenomena. Indeed, it is likely that a combination of various characteristics on the image is used to discriminate density. We discuss this in the next subsection;

2. The role of stereo is negligible. This might be due to the range of angles that we have chosen for the orientation distribution of the flakes. It could be too narrow to elicit sufficient binocular differences for the stereoscopic condition. This calls for further work to investigate this issue. Indeed we plan to combine head tracking and a smaller range of values for density in a future experiment. Stereo could have larger effects for larger binocular luminance differences;

3. The range of variations for the constant stimuli that we have chosen is at a too small scale to elicit a good measure of JND. The variations of the psychometric curves occur in the interval 30.8% to 29.1%, which comprises only 6 plates of different metallic flake density. To overcome this problem, one must increase the number of flake density variations in the interval 25% to 75%.

4.1 Metrics

As we have mentioned at the beginning of section 2.1.2 "Image Analysis", a single characteristic or most likely a combination of characteristics of the images can be used by the Human Visual System (HVS) to discriminate density. It can either be local properties (local gray level peak, specific sizes of clusters), but also a perception at the global scale of each image, which we will call "texture level" in this paper.

Two main behaviors were reported to be used by the subjects: Firstly, subjects reported to use a strategy of global visual appreciation and comparison of reference and stimulus image; They also reported a second strategy that used a focus on a specific area and by comparing this area on the two images (reference and stimuli). Finally, they also reported a combination of both.

The surface of the plate is characterized by a spatial distribution of punctual specular reflections, which gives rise to a visual contrast. Since the HVS is sensible to contrast variations. We can exploit this characteristic by

developing a metric based on contrast levels among flakes and background. However, it remains unclear how different variations of contrast influence the perceptive results.

During the experiment we noticed that the brightness of the area of the projection is not uniform. Using a projector at close distance to the screen is not an accurate solution to solve the problem. Even though we have a high dots per inch (DPI) level, it doesn't mean that we will have the same effects (sparkling, glittering) as in the real plate. The display can never mimic the physical interactions of light, as they are in real life. There is also a limitation of the high dynamic range of the luminosity of the display. That is, observing a plate in the display is different than observing a plate in the real world.

In this paper, thanks to granulometry study of the stimulus images, we have shown that a specific scale of clusters (opening 9-pixels) participates more strongly that others to gray level changes between different density stimuli.

The experiment was carried out using a a reference plate with a fixed value of 30.1%. However, it remains unclear the consequences of changing flake density of the reference plate on the perception thresholds.

4.2 Image Generation Model

As mentioned previously, we used a single Voronoï segmentation of 2D space for all stimuli, the consequence of this is that the position of all flakes and black background areas remains constant over all stimuli. This was done by choice. The other way around was to recreate a spatial distribution for each reference and stimulus densities. However in that case we were not sure of the perceptive similarity between two different spatial Voronoï distributions of equal densities. This strategy would have called for a pre-study to assess the perceptive similarity between series of equal density plates with different Voronoï distributions.

One might argue that this constant spatial distribution could have elicited an habituation effect during comparisons. By that we mean that some subjects could have memorized the spatial distribution of flakes and could have waited for the "apparition" or "disappearance" of flakes between the reference and the stimulus.

We believe though that is was not the case, first, because we tried to avoid this effect by displaying a black screen for 3 seconds between each test, in order to minimize the memorization. Secondly, no subjects reported to have recognized that the spatial distributions were the same.

However for future tests, we could avoid a pre-study by simply proposing rotated images between tests.

5. CONCLUSIONS

This work contributes to a better stereo visualization of goniochromatic materials within CG simulations. We provide perception thresholds and density metrics, which improve the understanding of limits of perception of flake density for stereoscopic and monoscopic display. Our work distinguish from the others in the sense that we study the perception thresholds for flake density.

We evaluate an heuristic metallic flake model under stereoscopic and monoscopic visualisations conditions. Then, we establish a link between the perception of the material to his virtual conception. Where we associate a human response of an optical signal to an physical identity. In other words, we correspond a perceptive metric (the 9-pixel opening) to the physical characteristics of the virtual plate. For that purpose, we used morphology image processing techniques. Where we identify which opening sizes the gray levels of the stimulus vary the most .

The obtained shows the combined role of flakes and background, but it is unclear if the stereoscopic effects are stemming only from flakes or also their surrounding background. To ensure that the perception thresholds remain consistent independently of the background, we are preparing a future experiment with different backgrounds.

We obtained small differences between the JNDs between the monoscopic and stereoscopic case. We think that using plates with more variations of flakes density could emphasize the discrimination between both JNDs.

A full characterization of the discrimination thresholds requires the knowledge of the weight of other visual cues on the observer perception. We are currently carrying studies about the influence of motion parallax on the perception of flake density. Another line of research is the role played by the background.

6. ACKNOWLEDGEMENTS

This work is part of the LIMA project (Light Interaction Material Aspect), which is a collaborative research project between academic researchers and industrial manufacturers. The project is funded by the French National Research Agency, ANR, with the Grant Number ANR-11-RMNP-0014. The authors wish to thank the persons who participated in the user study.

REFERENCES

[1] Wilkie, A., Weidlich, A., Magnor, M., and Chalmers, A., "Predictive rendering," in [*ACM SIGGRAPH ASIA 2009 Courses*], *SIGGRAPH ASIA '09*, 12:1–12:428, ACM, New York, NY, USA (2009).

[2] Escoda, J., Willot, F., Jeulin, D., Sanahuja, J., and Toulemonde, C., "Estimation of local stresses and elastic properties of a mortar sample by {FFT} computation of fields on a 3d image," *Cement and Concrete Research* **41**(5), 542 – 556 (2011).

[3] McCamy, C. S., "Observation and measurement of the appearance of metallic materials. part i. macro appearance," *Color Research and Application* **21**(4), 292–304 (1996).

[4] McCamy, C. S., "Observation and measurement of the appearance of metallic materials. part ii. micro appearance," *Color Research and Application* **23**(6), 362–373 (1998).

[5] Fettis, G., [*Automotive Paints and Coatings*], Wiley (2008).

[6] Nicodemus, F. E., Richmond, J. C., Hsia, J. J., Ginsberg, I. W., and Limperis, T., "Radiometry," ch. Geometrical Considerations and Nomenclature for Reflectance, 94–145, Jones and Bartlett Publishers, Inc., USA (1992).

[7] Boher, P., Leroux, T., and Bignon, T. *SID Conference Record of the International Display Research Conference* .

[8] Kook Seo, M., Yeon Kim, K., Bong Kim, D., and Lee, K. H., "Efficient representation of bidirectional reflectance distribution functions for metallic paints considering manufacturing parameters," *Optical Engineering* **50**(1), 013603–013603–12 (2011).

[9] Ďurikovič, R. and Martens, W. L., "Simulation of sparkling and depth effect in paints," in [*Proceedings of the 19th spring conference on Computer graphics*], *SCCG '03*, 193–198, ACM, New York, NY, USA (2003).

[10] Ershov, S., Ďurikovič;, R., Kolchin, K., and Myszkowski, K., "Reverse engineering approach to appearance-based design of metallic and pearlescent paints," *Vis. Comput.* **20**, 586–600 (Nov. 2004).

[11] Günther, J., Chen, T., Goesele, M., Wald, I., and Seidel, H.-P., "Efficient acquisition and realistic rendering of car paint," in [*Vision, Modelling, and Visualization 2005 (VMV), Proceedings, November 16-18, Erlangen, Germany*], Greiner, G., Hornegger, J., Niemann, H., and Stamminger, M., eds., 487–494, Akademische Verlagsgesellschaft Aka GmbH, Berlin (November 2005).

[12] Rump, M., Mller, G., Sarlette, R., Koch, D., and Klein, R., "Photo-realistic rendering of metallic car paint from image-based measurements," *Computer Graphics Forum* **27**(2), 527–536 (2008).

[13] Sung, L., Nadal, M. E., McKnight, M. E., Marx, E., and Dutruc, R., "Effect of aluminum flake orientation on coating appearance.," 1–15 (2001).

[14] Zhao, Y., Chen, Z., Zhu, C., Tan, Y.-P., and Yu, L., "Binocular just-noticeable-difference model for stereoscopic images," *Signal Processing Letters, IEEE* **18**(1), 19–22 (2011).

[15] LEVELT, W. J. M., "Binocular brightness averaging and contour information," *British Journal of Psychology* **56**(1), 1–13 (1965).

[16] Ged, G., Obein, G., Silvestri, Z., Le Rohellec, J., and Vinot, F., "Recognizing real materials from their glossy appearance," *Journal of Vision* **10**(9) (2010).

[17] Obein, G., Knoblauch, K., and Viénot, F., "A framework for the measurement of visual appearance.," *Commission Internationale de l'Eclairage (CIE)* **4**, 711–720 (Aug. 2006).

[18] Templin, K., Didyk, P., Ritschel, T., Myszkowski, K., and Seidel, H.-P., "Highlight microdisparity for improved gloss depiction," *ACM Trans. Graph.* **31**, 92:1–92:5 (July 2012).

[19] Wendt, G., Faul, F., and Mausfeld, R., "Highlight disparity contributes to the authenticity and strength of perceived glossiness," *Journal of Vision* **8**(1) (2008).

[20] Obein, G., Knoblauch, K., and Viénot, F., "Difference scaling of gloss: nonlinearity, binocularity, and constancy.," *Journal of vision* **4**, 711–720 (Aug. 2004).

[21] Sakano, Y. and Ando, H., "Effects of head motion and stereo viewing on perceived glossiness," *Journal of Vision* **10**(9), 1–14 (2010).

[22] David C. Knill, J. A. S., "Do humans optimally integrate stereo and texture information for judgments of surface slant?," (2003).

[23] Weidlich, A. and Wilkie, A., "Modeling aventurescent gems with procedural textures," in [*Proceedings of the 24th Spring Conference on Computer Graphics*], *SCCG '08*, 51–58, ACM, New York, NY, USA (2010).

[24] De Coster, M. and Chermant, J., [*Précis d'analyse d'images*], CNRS plus, Centre National de la Recherche Scientifique (1989).